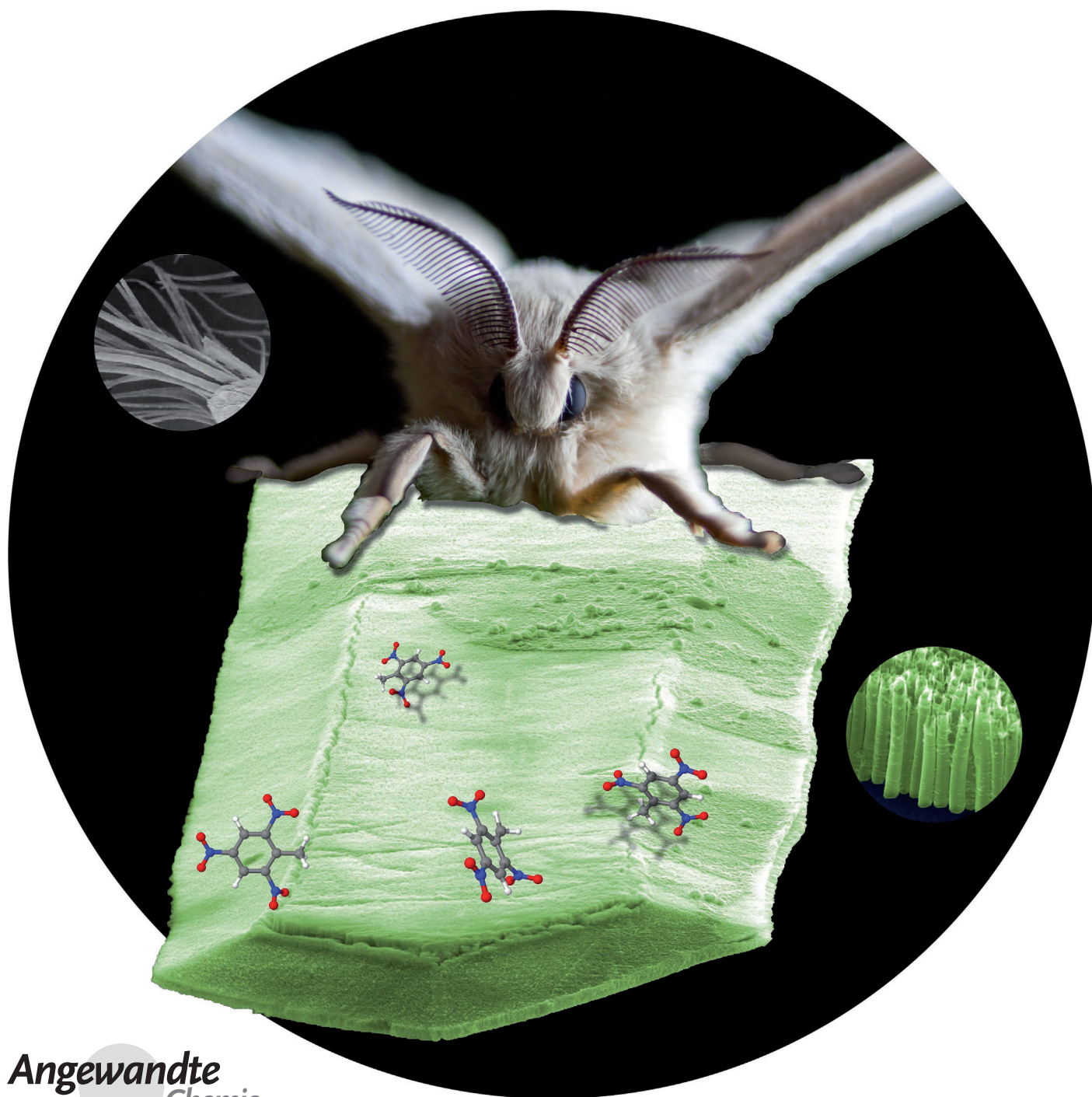


# Bio-Inspired Nanostructured Sensor for the Detection of Ultralow Concentrations of Explosives\*\*

*Denis Spitzer, Thomas Cottineau, Nelly Piazzon, Sébastien Josset, Fabien Schnell, Sergey Nikolayevich Pronkin, Elena Romanovna Savinova, and Valérie Keller\**



Micromechanical sensors based on microcantilevers with piezoresistive or optical signal detection have recently opened new perspectives for the detection of different chemicals (toxic metal ions, volatile organics, explosives, etc.).<sup>[1]</sup> Optical detection in dynamic mode (i.e. by following the resonant frequency shift of a microcantilever) is expected to result in especially low detection limits.<sup>[2]</sup> Unfortunately, the sensitivity of these micromechanical devices is limited by their small surface area. This insufficient sensitivity is one of the main constraints for the detection of airborne compounds at low concentrations. Several attempts have been made to increase the surface area, mainly by roughening or by coating with porous gels or tangled wires.<sup>[3]</sup>

Owing to the low volatilities of explosives at ambient conditions, their detection remains a major challenge, and the existing methods are unable to simultaneously meet the requirements of portability, sensitivity, and analysis speed.<sup>[4]</sup> To date, despite numerous limitations, dogs remain one of the most efficient sensing systems.<sup>[5]</sup> The detection of explosive vapors using the resonant frequency shift caused by adsorption and an induced thermal decomposition of trinitrotoluene (TNT) was reported by Thundat et al. for an uncoated microcantilever.<sup>[6]</sup> Subsequent studies were devoted to the functionalization of microcantilevers with organic molecules for increasing the strength of their interaction with the explosives, and the detection limit of 10–30 parts per trillion (ppt) was achieved.<sup>[7]</sup>

Inspired by the structure of the sensing system of some moth species able to detect single pheromone molecules, we demonstrate that modifying a silicon microcantilever with a three-dimensionally ordered layer of vertically aligned titania nanotubes (TiO<sub>2</sub>-NTs) makes it possible to lower the TNT detection threshold down to the ppt range. This approach combines the high sensitivity of micromechanical cantilevers in dynamic mode with the attractive properties of ordered TiO<sub>2</sub>-NT nanostructures,<sup>[8]</sup> namely 1) their high surface area, 2) the high affinity of TiO<sub>2</sub> to nitro compounds, and 3) the open structure of TiO<sub>2</sub>-NTs which facilitates mass transport and thus results in fast sensor response.

Herein we report for the first time on the synthesis of highly ordered TiO<sub>2</sub>-NT arrays on cantilevers with a micrometric surface area. To achieve these architectures, we developed a two-step procedure consisting of the physical

vapor deposition (PVD) of a dense layer of Ti metal onto a silicon microcantilever followed by its anodization in a fluoride-containing electrolyte.<sup>[9]</sup> The titanium anodization process developed by Zwilling and co-workers<sup>[10]</sup> forms oriented metal oxide nanotube arrays supported on a metal surface, and can be employed in a wide range of applications such as photovoltaics, H<sub>2</sub> detection, and photocatalysis.<sup>[11–13]</sup> Recently, to broaden the range of applications, the anodization method has been extended to foreign substrates. Starting from a metallic titanium layer deposited by PVD methods, TiO<sub>2</sub>-NT arrays have been grown on a large-area silicon wafer, on FTO glass, and on graphene sheets.<sup>[14]</sup>

In the present work, the two steps of the synthesis were adapted to the specificity of the silicon cantilever substrate, that is, its small dimensions—(225 ± 10) μm length, (28 ± 7) μm width, and (3 ± 1) μm thickness—and the sensitivity to the fluoride attack.

The deposition parameters were optimized in order to obtain a dense layer of titanium (1 μm thick) with large grains, which is necessary for the subsequent formation of TiO<sub>2</sub>-NTs by anodization.<sup>[15]</sup> Then, the challenge was to anodize the layer of titanium preserving the transduction properties of the microcantilever. The anodization was performed in a glycerol-based electrolyte, and the experimental conditions were thoroughly optimized to achieve microcantilevers fully (rather than partially) covered on one side with aligned titania nanotubes (cf. SEM images in Figure 1 D–G). The key parameters optimized in this step were the anodization duration, the electrolyte composition, and the temperature. The anodization was limited to 2 h. This was necessary to preserve a film of metallic Ti, with the thickness sufficient for ensuring the integrity of the TiO<sub>2</sub>-NT layer and its bonding to the Si substrate.

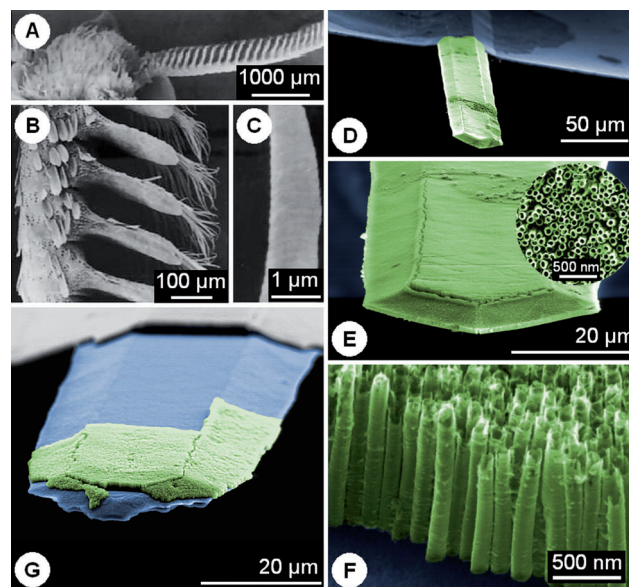


**Figure 1.** A–C) Sensing system of the silkworm *Bombyx mori* showing micrometer-sized sensilla grafted to antennae (reproduced from Ref. [16]). D–F) Nanostructured microcantilever covered by TiO<sub>2</sub>-NTs. G) Microcantilever partially covered by TiO<sub>2</sub>-NTs obtained by anodization under unoptimized conditions.

[\*] Dr. D. Spitzer, Dr. N. Piazzon, Dr. S. Josset, F. Schnell  
NS3E-ISL-CNRS (Nanomatériaux pour les Systèmes Sous  
Sollicitations Extrêmes) UMR 3208

French–German Research Institute of Saint-Louis

5 rue du Général Cassagnou, B.P. 70034

68301 St Louis Cedex (France)

and

Postfach 1260, 79574 Weil am Rhein (Germany)

Dr. T. Cottineau, Dr. S. N. Pronkin, Prof. E. R. Savinova, Dr. V. Keller

LMSPC-CNRS-UDS (Laboratoire des Matériaux, Surfaces

et Procédés pour la Catalyse) UMR 7515

25 rue Becquerel, 67087 Strasbourg Cedex (France)

[\*\*] This work was supported by DGA contract no. 2009.34.0024. We thank Dr. M. Rosenthal and Dr. D. A. Ivanov for the system combining nanocalorimeter with AFM, and C. Meny and M. Acosta for their help with the PVD.



The glycerol-based electrolyte and the anodization temperature were both optimized to limit the dissolution of silicon by controlling the viscosity of the medium, and thus the fluoride diffusion. The nanotubes grown with the optimized protocol (see the Experimental Section for more details) have a length of  $(1700 \pm 50)$  nm, an external diameter of  $(100 \pm 5)$  nm, and a wall thickness of  $(20 \pm 5)$  nm. The density of the tube “forest” on the substrate is approximately  $8 \times 10^9 \text{ cm}^{-2}$ , corresponding to ca. 500 000 nanotubes per microcantilever (in comparison, the silkworm *Bombyx mori* has between 600 and 900 sensilla on the surface of the antennal branches of one of its antennae; see Figure 1 A–C). The presence of  $\text{TiO}_2$ -NTs on the silicon cantilever surface increases the surface area by a factor of 80. This value was estimated from the calculated surface area of titania nanotubes and the surface of the microcantilever.

The possibility of using these nanostructured microcantilevers to detect explosives was tested by generating pulses of TNT vapor and recording the frequency shift of the microcantilever. For this purpose, a single TNT microcrystal was placed on a nanocalorimeter chip below a microcantilever and heated to  $47^\circ\text{C}$  (Figure 2B). It is worth mentioning that the device was tested under ambient atmosphere thus emulating detection under real-life conditions (possible exposure to pollutants and humidity; see Figure 2A). To exclude condensation of the vapors, which is of little interest for detection purposes, the microcantilever was maintained at a slightly higher temperature ( $50^\circ\text{C}$ ) than the vapor source. Under these conditions, no shift of the resonant frequency was detected on the pristine (unmodified) microcantilever. For a microcantilever covered with a film of metallic Ti (obtained after Ti sputtering but before the anodization) only a small shift of 2.5 Hz (see insert in Figure 3) was observed. In contrast, a significant downshift of 250 Hz with a decrease rate of  $85.6 \text{ Hz min}^{-1}$  (95 % confidence interval:  $\pm 1.5 \text{ Hz min}^{-1}$ ) was measured over approximately 3 min on the nanostructured microcantilever, without showing any saturation (Figure 3). It is noteworthy that once exposed to the ambient atmosphere, titanium metal is almost instantaneously passivated with an oxide layer a few nanometers thick; hence the chemical nature of the cantilever sputtered with Ti is similar to that of  $\text{TiO}_2$ -NT. The two orders of magnitude difference in the frequency shift is in agreement with the expected surface enhancement resulting from the nanostructuring. The short-term stability of the resonant frequency response in these experiments is only about 0.36 Hz (three times the standard deviation of the noise level), even when the experiments were performed under real-life conditions.

In order to determine the TNT concentration in air at a given distance  $R$  from its solid source, we adopt the procedure of Gershanik and Zeiri<sup>[17]</sup> and assume that molecular diffusion is the dominating transport process, while other phenomena, like convection, are negligible. We consider diffusion under steady-state conditions when mass accumulation is zero<sup>[18]</sup> and use the Fick’s first law of diffusion with the following boundary conditions:

- the gas phase adjacent to the particle (radius  $30 \mu\text{m}$ ) surface is saturated with the explosive (vapor pressure of

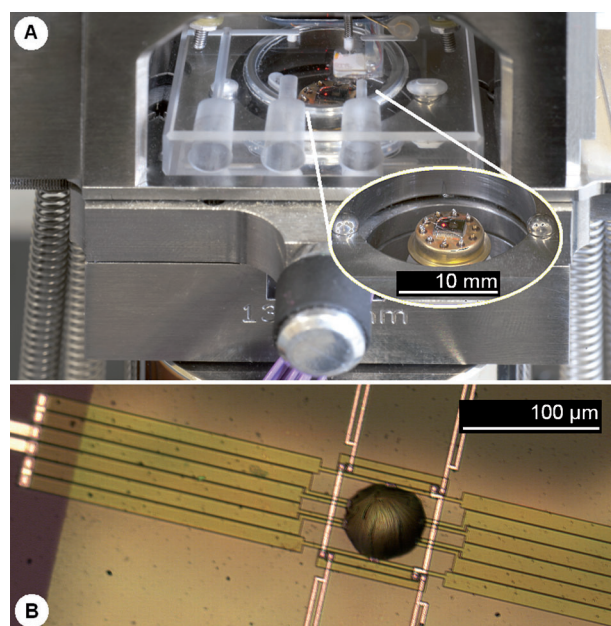


**Figure 2.** A) Nanocalorimetric chip placed in the AFM with and without the cantilever above the chip (experiments were performed under ambient conditions). B) Hemispherical TNT particle loaded on the heatable membrane of a nanocalorimeter to generate pulses of ultra-low concentrations of the explosive vapor.

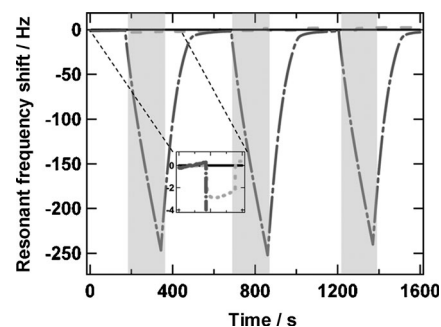


**Figure 3.** Resonant frequency shifts of a pristine microcantilever (—), one covered with titanium and its native oxide layer (----), and one nanostructured with  $\text{TiO}_2$ -NTs (-.-) submitted to intermittent pulses of explosive vapor (gray zones). The insert is an enlargement for  $0 < t < 400$  s and  $-4 < \Delta f < 0$  Hz. The cantilevers were at  $50^\circ\text{C}$  and TNT was heated to  $47^\circ\text{C}$  under quasi-isothermal conditions.

TNT according to Oxley et al.: 3 MPa corresponding to 29.6 ppb at  $47^\circ\text{C}$ ).<sup>[19]</sup>

- the concentration of TNT far away from the particle is zero.

This leads to the concentration profile  $C^{\text{TNT}}(R, R_0, T)$  described by Equation (1) as detailed in reference [18].

$$C^{\text{TNT}}(R, R_0, T) = C_{\text{Sat}}^{\text{TNT}}(T) \frac{R_0}{R} \quad (1)$$

Here  $C_{\text{Sat}}^{\text{TNT}}$  is the saturated concentration of TNT at temperature  $T$ ,  $R_0$  is the radius of the hemispherical particle, and  $R$  is the distance between the particle and the cantilever. Application of Equation (1) suggests that the microcantilever is

exposed to a concentration not exceeding 530 ppt.

Consequently, considering the signal-to-noise ratio, a resonant frequency shift of 250 Hz at a TNT concentration of 530 ppt over a duration of 3 min (chosen for detection under realistic conditions) implies that the detection threshold of this bio-inspired sensor can be estimated to be below 1 ppt within roughly 3 min, an unprecedented value for microcantilevers.<sup>[6]</sup> Moreover, the excellent reversibility and repeatability of the adsorption–desorption process is proven. These results prove unambiguously that TNT strongly interacts with the surface of the TiO<sub>2</sub>-NTs. Furthermore, the use of quasi-isothermal detection conditions ensures for the first time that the observed variation of the resonant frequency is due to adsorption from the gas phase and not condensation occurring on any surface at a temperature lower than that of the explosive vapor source.

The selectivity of the microcantilever covered with TiO<sub>2</sub>-NTs was tested with ethanol and heptane vapors at concentrations of  $\delta = 6.4 \times 10^2$  and  $6.8 \times 10^2$  ppm, respectively. It should be noted that these concentrations are much higher (four orders of magnitude) than that used in the case of TNT ( $\delta = 0.03$  ppm). We have chosen ethanol to illustrate the effect of alcohol vapors, which could be present in airports, and heptane, which is a common component of gasoline. The relative responses of the microcantilever system to these three analytes under the established experimental conditions are depicted in Figure 4. We do not observe any frequency shift for ethanol and a very low one for heptane. It is well known that compounds with NO<sub>2</sub> groups have a good affinity to TiO<sub>2</sub>. According to some publications, TiO<sub>2</sub> is used as a sensing material for NO<sub>2</sub> groups.<sup>[20,21]</sup> The lower response to the other compounds can be explained by a lower affinity for TiO<sub>2</sub> at 50°C.

In conclusion, we have shown that the detection capacities of microcantilever-based systems can be greatly enhanced by three-dimensional nanostructuring. The combination of organized three-dimensional nanostructures with a high affinity toward explosives and an efficient transducing system like a microcantilever represents a breakthrough in the detection of explosives in the vapor phase. This is the first

report in which microcantilevers have been functionalized with an open three-dimensional nanostructure inspired by a unique sensing system from nature. While this work demonstrates the feasibility and the promise of the approach, further research and development is required to build a functional device. For practical applications it is vitally important to enhance the selectivity towards other kinds of organic vapors that could be present in real atmospheres, but also to distinguish between different kinds of explosives. Such studies are underway and rely on the surface functionalization of TiO<sub>2</sub>-NTs with specific organic functional groups or biomolecules. The final goal would be the integration of different microcantilevers in a polyvalent artificial electronic nose to contribute to global security. Thanks to the thermal stability of the TiO<sub>2</sub>-NTs, the decomposition of the adsorbed material could be a very interesting way to distinguish between energetic and inert materials. Because of the versatility of the nanostructuring approach, it could easily be transposed to enhance the detection sensitivity towards other kinds of chemicals at very low concentrations, for instance for sensing different organic pollutants.

### Experimental Section

**TiO<sub>2</sub>-NTs for nanostructuring the microcantilever:** In order to obtain nanostructured microcantilevers covered by TiO<sub>2</sub>-NTs, the silicon microcantilevers (TL-FM, Nanosensors) were cleaned for 5 min successively in acetone, ethanol, and ultrapure water, and then dried under an N<sub>2</sub> flux. After this cleaning procedure the samples were quickly attached to the sample holder of a DC magnetron sputtering system with a titanium target (MaTeck, 99.99%). The system was pumped down to  $4.8 \times 10^{-7}$  Pa. The substrate surface was etched with Ar plasma for 30 s. Then film deposition was carried out in a  $20 \text{ cm}^3 \text{ min}^{-1}$  flux of argon, and a plasma current of 800 mA. The samples were heated to 50°C and the deposition duration was adjusted to achieve a film thickness of roughly 1  $\mu\text{m}$ . Thereafter, silicon microcantilevers covered with the titanium film were immersed in aqua regia (HCl/HNO<sub>3</sub> 3:1) for 3 min, rinsed with water, and dried under N<sub>2</sub>. After consecutive cleaning steps in acetone, ethanol, and water baths, and drying under an N<sub>2</sub> flux, the samples were mounted in the anodization sample holder. The anodization was performed in a two-electrode configuration with a platinum counterelectrode. The Teflon electrochemical cell was placed in a cryothermostat to maintain the electrolyte temperature at  $(27 \pm 1)^\circ\text{C}$  during the anodization. The electrolyte was glycerol (purity  $\geq 99.5\%$ ) containing 2 vol% ultrapure H<sub>2</sub>O and 0.5 wt% ammonium fluoride (purity  $\geq 98\%$ ). All chemicals are from Sigma–Aldrich and used without further purification. The voltage between the two electrodes was progressively increased from 0 to 35 V with a ramp of  $20 \text{ mV s}^{-1}$ , and then kept at a constant value of 35 V for at most 2 h. After the anodization, samples were thoroughly rinsed with ultrapure water to remove glycerol and ammonium fluoride from the tubular structure and then dried under a gentle N<sub>2</sub> flux.

**Generation and detection of explosive vapor:** A heatable nanocalorimeter chip (Xensor Integration) was utilized to generate pulses of ultralow traces of explosive vapors under controlled and repeatable conditions.<sup>[22]</sup> A TNT microcrystal was loaded on the chip and was first melted by a 100 ms heat pulse at 100°C to obtain a hemispheric shape and to ensure excellent thermal contact with the nanocalorimeter membrane (Figure 2B). The solid explosive sample was placed above at a constant distance (1700  $\mu\text{m}$ ) from the sensing microcantilever in an AFM Multimode head (Veeco) combined with a “phase-locked-loop” system (Nanonis) that recorded the microcantilever resonant frequency. The ethanol and heptane pulses were produced

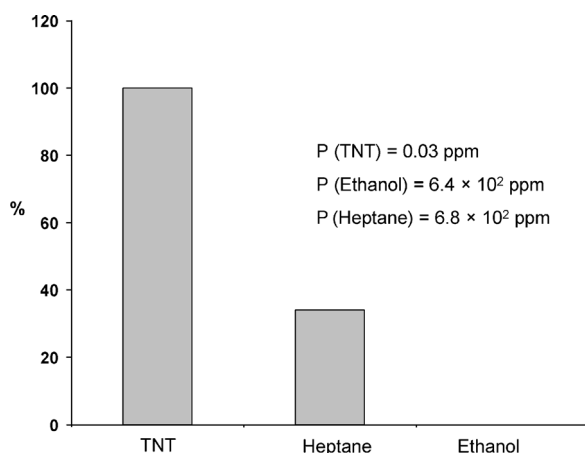


**Figure 4.** Relative responses of the cantilever covered with TiO<sub>2</sub>-NTs to TNT, heptane, and ethanol.

using an air stream saturated with analyte at  $-12^{\circ}\text{C}$ . The analytes were ethanol and *n*-heptane with purities of 99.9% and 99.7%, respectively (GPR RECTAPUR).

Received: November 23, 2011

Revised: March 15, 2011

Published online: April 27, 2012

**Keywords:** analytical methods · explosive detection · microcantilevers · sensors

- [1] a) K. M. Goeders, J. S. Colton, L. A. Bottomley, *Chem. Rev.* **2008**, *108*, 522; b) A. B. Boisen, S. Dohn, S. S. Keller, S. Schmid, M. Tenje, *Rep. Prog. Phys.* **2011**, *74*, 036101.
- [2] L. G. Carrascosa, M. Moreno, M. Alvarez, L. M. Lechuga, *TrAC Trends Anal. Chem.* **2006**, *25*, 196.
- [3] a) J. J. Headrick, M. J. Sepaniak, N. V. Lavrik, P. G. Datskos, *Ultramicroscopy* **2003**, *97*, 417; b) D. Lee, E.-H. Kim, M. Yoo, N. Jung, K.-H. Lee, S. Jeon, *Appl. Phys. Lett.* **2007**, *90*, 113107.
- [4] D. S. Moore, *Rev. Sci. Instrum.* **2004**, *75*, 2499.
- [5] R. J. Colton, J. N. Russel, Jr., *Science* **2003**, *299*, 1324.
- [6] a) L. A. Pinnaduwa, A. Gehl, D. L. Hedden, G. Muralidharan, T. G. Thundat, R. T. Lareau, T. Sulchek, L. Manning, B. Rogers, M. Jones, J. D. Adams, *Nature* **2003**, *425*, 474; b) T. G. Thundat (Lockheed Martin Energy Research Corporation), US Patent 5918263, **1999**.
- [7] a) L. A. Pinnaduwa, V. Boiadjev, J. E. Hawk, T. G. Thundat, *Appl. Phys. Lett.* **2003**, *83*, 1471; b) G. M. Zuo, X. X. Li, Z. X. Zhang, T. T. Yang, Y. L. Wang, Z. X. Cheng, S. L. Feng, *Nanotechnology* **2007**, *18*, 255501.
- [8] a) S. Banerjee, S. K. Mohapatra, M. Misra, I. B. Mishra, *Nanotechnology* **2009**, *20*, 075502; b) M. Boehme, F. Voelklein, W. Ensinger, *Sens. Actuators B* **2011**, *158*, 286.
- [9] P. Roy, S. Berger, P. Schmuki, *Angew. Chem.* **2011**, *123*, 2956; *Angew. Chem. Int. Ed.* **2011**, *50*, 2904.
- [10] V. Zwillig, M. Aucouturier, E. Darque-Ceretti, *Electrochim. Acta* **1999**, *45*, 921.
- [11] O. K. Varghese, M. Paulose, C. A. Grimes, *Nat. Nanotechnol.* **2009**, *4*, 592.
- [12] C. Ruan, M. Paulose, O. K. Varghese, G. K. Mor, C. A. Grimes, *J. Phys. Chem. B* **2005**, *109*, 15754.
- [13] a) J. M. Macak, H. Tsuchiya, L. Taveira, S. Aldabergerova, P. Schmuki, *Angew. Chem.* **2005**, *117*, 7629; *Angew. Chem. Int. Ed.* **2005**, *44*, 7463; b) O. K. Varghese, M. Paulose, T. J. LaTempa, C. A. Grimes, *Nano Lett.* **2009**, *9*, 731.
- [14] a) J. M. Macak, H. Tsuchiya, S. Berger, S. Bauer, S. Fujimoto, P. Schmuki, *Chem. Phys. Lett.* **2006**, *428*, 421; b) G. K. Mor, O. K. Varghese, M. Paulose, C. A. Grimes, *Adv. Funct. Mater.* **2005**, *15*, 1291; c) T. Cottineau, I. Janowska, N. Macher, D. Bégin, M. J. Ledoux, S. Pronkin, E. Savinova, N. Keller, V. Keller, C. Pham-Huu, *Chem. Commun.* **2012**, *48*, 1224.
- [15] K. Kalantar-Zadeh, A. Z. Sadek, H. Zheng, J. G. Partridge, D. G. McCulloch, Y. X. Li, X. F. Yu, W. Wlodarski, *Appl. Surf. Sci.* **2009**, *256*, 120.
- [16] J. F. Picimbon, *Med. Sci.* **2002**, *18*, 1089.
- [17] A. P. Gershanik, Y. Zeiri, *J. Phys. Chem. A* **2010**, *114*, 12403.
- [18] E. L. Cussler, *Diffusion: mass transfer in fluid systems*, Cambridge Univ. Press, Cambridge, **1997**, p. 39.
- [19] J. C. Oxley, J. L. Smith, K. Shinde, J. Moran, *Propellants Explos. Pyrotech.* **2005**, *30*, 127.
- [20] D. Wang, A. Chen, S.-H. Jang, H.-L. Yip, A. K.-Y. Jen, *J. Mater. Chem.* **2011**, *21*, 7269.
- [21] J. A. Rodriguez, T. Jirsak, G. Liu, J. Hrbek, J. Dvorak, A. Maiti, *J. Am. Chem. Soc.* **2001**, *123*, 9597.
- [22] N. Piazzon, M. Rosenthal, A. Bondar, D. Spitzer, D. A. Ivanov, *J. Phys. Chem. Solids* **2010**, *71*, 114.